Electronic Degeneracy and Vibrational Degrees of Freedom: The Permutational Proof of the Jahn–Teller Theorem

Arnout Ceulemans and Erwin Lijnen

Abstract In 1937 Jahn and Teller stated their remarkable theorem that all non-linear nuclear configurations are unstable for an orbitally degenerate electronic state. The original demonstration of this theorem was by exhaustive verification for all non-trivial cases. Since then several authors have presented theoretical treatments that offer formal proofs. None of these however succeeds to attain a real insight into the origin of the theorem, nor does there appear to exist a general proof that covers all point groups in a uniform way. For a clear understanding of the Jahn–Teller theorem a different starting point is needed, based on the question: What is the origin of electronic degeneracy? According to Group Theory the existence of an $n-1$ fold degeneracy is related to the existence of a set of n identical sites which form a doubly transitive orbit of a symmetry group. Using the symmetric groups this permutational character of electronic degeneracies can be turned into a transparent proof for the Jahn–Teller theorem. The presentation of this proof is preceded by introductory sections which explain the principal group-theoretical concepts that come into play. The proof is followed by an application to the fivefold degenerate irreducible representation in the icosahedral group. This quintuplet degeneracy can be described by the S_6 permutation group, which gives rise to extra selection rules. The embedding of the icosahedral group in S_6 is discussed, and the relevance of this group-theoretical scheme for the Jahn–Teller interactions in icosahedral shells is demonstrated. The extension to the hyperoctahedron in 4D space is also discussed.

1 Introduction

The Jahn–Teller theorem states that 'a configuration of a polyatomic molecule for an electronic state having orbital degeneracy cannot be stable with respect to all displacements of the nuclei unless in the original configuration all the nuclei lie on a straight line' [1]. In the original paper of 1937 verification of the theorem was by enumeration of all possible cases. In the words of Teller, 'this was not a proof that a

mathematician would enjoy.'[1] Nevertheless up till now the original procedure is still considered to be the most practical and useful way to introduce the theorem [2]. Several authors have presented more general proofs, which however lack transparency and do not yield additional insights into the strong connection between distortions and degeneracy. In the present paper we will first review these treatments and then develop a different point of view which leads to a concise permutational proof.

2 Existing Proofs of the Jahn–Teller Theorem

The first attempt to clarify the physical basis of the Jahn–Teller theorem was due to Ruch, [3] in an introductory presentation to the 1957 annual meeting of the Bunsen–Gesellschaft in Kiel, which was organised by H. Hartmann. Ruch discussed the general connection between symmetry and chemical bonding, and also touched upon the Jahn–Teller effect in transition-metal complexes. He explained that degeneracy can always be related to the existence of a higher than twofold rotational axis and a wave function which is not totally symmetric under a rotation around this axis. Provided that the wave function is real the electron densities for such a wave function are bound to be anisotropic. The combination of an anisotropic distribution of the electron cloud and a symmetric nuclear frame leads to electrostatic distortion forces where the nuclear frame adapts itself to the anisotropic attraction force.

Strictly speaking the densities of the electronic cloud on the sites of the atomic nuclei, the so-called *on-site* density, need not be different for different components of a degenerate wave function. A simple counter-example is a T_{1u} orbital level in a cubic cluster. Let $|\sigma_i\rangle$ denote a σ-type atomic orbital on a given site i. The symmetry adapted linear combinations (SALC's) of these basis orbitals are given by (see Fig. 1):

$$
\begin{aligned}
|T_{1u}x> &= \frac{1}{2\sqrt{2}}\left(|\sigma_1\rangle - |\sigma_2\rangle - |\sigma_3\rangle + |\sigma_4\rangle + |\sigma_5\rangle + |\sigma_6\rangle - |\sigma_7\rangle - |\sigma_8\rangle\right) \\
|T_{1u}y> &= \frac{1}{2\sqrt{2}}\left(|\sigma_1\rangle + |\sigma_2\rangle - |\sigma_3\rangle - |\sigma_4\rangle - |\sigma_5\rangle + |\sigma_6\rangle + |\sigma_7\rangle - |\sigma_8\rangle\right) \\
|T_{1u}z> &= \frac{1}{2\sqrt{2}}\left(|\sigma_1\rangle + |\sigma_2\rangle + |\sigma_3\rangle + |\sigma_4\rangle - |\sigma_5\rangle - |\sigma_6\rangle - |\sigma_7\rangle - |\sigma_8\rangle\right). \quad (1)
\end{aligned}
$$

Clearly all three components have the same on-site densities. What differs are the *inter-site* or overlap matrix elements. The importance of these inter-site contributions is confirmed by a recent analysis of the vibronic coupling density functional [4]. Parenthetically we note that a function which has the same on-site

[1] Historical note by Edward Teller in R. Englman, *The Jahn–Teller effect in molecules and crystals* (Wiley, London, 1972). See also: B. R. Judd, in: *Vibronic Processes in Inorganic Chemistry,* C. D. Flint (ed.) Nato ASI series C288, pp. 79–101 (Kluwer, Dordrecht, 1989)

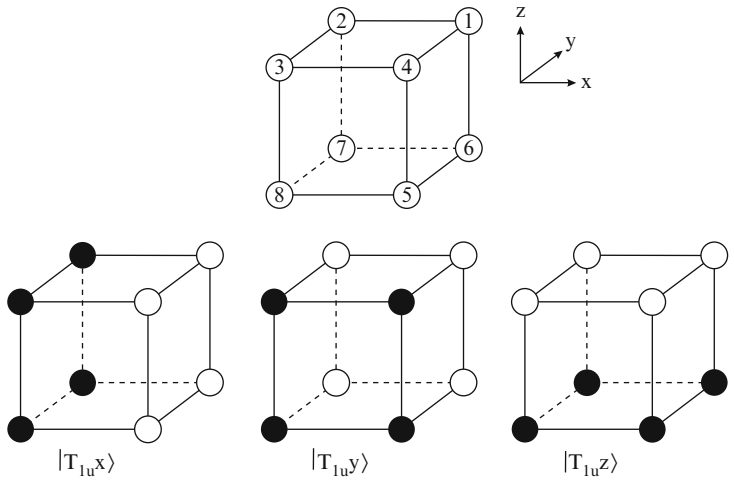

Fig. 1 SALC's for the T_{1u} representation of the cube

density on all equivalent atomic sites is called 'equidistributive'. In fact as we have shown elsewhere, [5] for all degeneracies of the cubic groups a degeneracy basis can always be constructed with equidistributive components, provided the use of complex component functions is allowed. For some icosahedral degeneracies more intricate cases may occur where the wave functions have to be of quaternionic form.

In 1968 Ruch and Schönhofer cast the qualitative arguments in a more formal proof [6]. The authors expressed the hope that the proof would yield additional insight. This hope did not really materialize because the proof was not very transparent, one of the reasons being that it was not illustrated with an actual example. In order to obtain a better understanding of this proof we try to apply it to a practical example of a ${}^2T_{2g}$ state in an octahedral complex, as would be the case for a $(d)^1$ transition-metal ion such as Ti^{3+} surrounded by six ligands. The site symmetry group of a ligand in an octahedron is C_{4v}. In this site symmetry group the T_{2g} symmetry of the electronic level transforms as $B_2 + E$. The argument then runs as follows: since the electronic level is threefold degenerate and the site-symmetry group only allows non-degenerate and twofold degenerate irreducible representations at least one of the components of the electronic level has to transform as a non-degenerate irreducible representation of the site group. This is indeed the case for the B_2 representation. The electronic density at the site transforms as the direct product $B_2 \otimes B_2 = A_1$ and thus is totally symmetric. This implies that the electronic level will always yield a non-zero vibronic coupling matrix element with the radial displacement of the ligand at that site. The proof continues to show that this condition is sufficient to claim vibronic instability of the octahedral triplet level. The radial distortions of the octahedron induce a distortion space of the following symmetry:

$$\Gamma\,(A_1\ C_{4v} \uparrow O_h) = a_{1g} + t_{1u} + e_g. \tag{2}$$

According to the Jahn–Teller theorem the active modes for an orbital multiplet are given by the non-totally symmetric part of the symmetrized direct product of the electronic degeneracy:

$$[T_{2g} \otimes T_{2g}] - a_{1g} = e_g + t_{2g}. \tag{3}$$

Square brackets denote the symmetrized part of the direct square. Two aspects of the formal proof are noteworthy. Firstly, as in the qualitative argument the proof only considers the on-site densities. As a result for the T_{2g} level the vibronic coupling resides with the radial distortions of the octahedron only, as described by the antisymmetric stretch of e_g symmetry which is the common symmetry in the above equations. However the 1937 Jahn–Teller treatment yielded a stronger result in that it showed *both* active modes to be present in an octahedral complex with six ligands. As we know T_{2g} electrons preferentially couple with tangential bending modes of t_{2g} symmetry rather than with radial e_g distortions, which coincide with nodal planes of the T_{2g} orbitals. Secondly, although the derivation is no longer by discrete enumeration the proof still rests on the consideration of several separate cases, depending on whether the index n in the cyclic site group C_{nv} is equal to 2 or larger than two, and whether the electronic degeneracy is even or odd.

In 1971 a different proof was provided by Blount in the Journal of Mathematical Physics [7]. Blount mentions that after the completion of his proof he learned about the work of Ruch and Schönhofer. He further notes that, although both treatments are closely connected, his approach 'uses the basic ideas in a more direct fashion and reveals more clearly the distinction between general and special features' (quoted from [7]). Indeed the 1971 proof calculates directly by means of the standard character theory the overlap between the direct square of the electronic irrep and the normal distortion modes. In line with Ruch and Schönhofer, Blount also subduces this expression to the site groups which leave individual atoms invariant. The proof then splits into several cases depending on whether the subduction of the electronic irrep is reducible or not. The irreducible case occurs when the atoms are lying on a threefold axis and urges Blount to consider the cubic and icosahedral groups separately. Interestingly Blount has also considered possible symmetry breaking in higher dimensions. He argued that already in 4D there appear symmetries where the JT theorem is not obeyed. We will illustrate an example of the hypercube in more details later. This may not be too surprising in view of the fact that also linear 1D structures constitute exceptions to the theorem.

Further rather indirect proofs have been given by Raghavacharyulu [8] and most recently by Pupyshev [9].

In the present work we will approach the problem from a different point of view, and start from the causes for electronic degeneracies. So we will ask ourselves the question: *Why is it that certain point groups contain degenerate irreps?* According to group theory the necessary and sufficient condition is that the group has at least two generators which do not commute. For a proper understanding of the Jahn–Teller effect this algebraic condition is not very useful, and we will find a

more inspiring answer in the theory of induction. Before we can proceed to the actual proof, we collect various group-theoretical propositions that will introduce the reader to the necessary mathematical background that is required for the subsequent proof. For a more intuitive chemical perspective on the present proof, we refer the interested reader to our recent contribution to the commemorative accounts of the Chemical Society of Japan [10].

3 Group-Theoretical Propositions

3.1 Transitive Left Cosets

Degeneracy starts from equivalence. A simple way to demonstrate that two objects are equivalent is when the permutation of the two objects is symmetry allowed. Consider a simple triatomic molecule with the shape of a regular triangle. The relevant point group in two dimensions is limited to C_{3v}. The equivalence of the three nuclei is demonstrated by symmetry operations which permute nuclei that are identical and occupy equivalent positions in space. The set of the three nuclei that are connected in this way is called an *orbit*. Symmetry operations are said to act *transitively* on the elements of the orbit, i.e. they send every element over into every other element of the same orbit. The *stabilizer* of a given nucleus $\langle a \rangle$ in the molecule is the subgroup $H_a \subset G$ which leaves the site $\langle a \rangle$ invariant. In the case of a triangle the stabilizer of a nucleus is a C_s subgroup. This corresponds to the site groups in the previous proofs. The total group may be expanded in left cosets of this subgroup, according to the general formula:

$$G = \sum_r g_r H, \tag{4}$$

where g_r is a coset generator or representative. The number of cosets is equal to the quotient of the group orders, $n = |G|/|H| = 3$. For our example, using the notation in Fig. 2 the coset expansion of C_{3v} over C_s reads:

$$C_{3v} = \{E, \sigma_a\} + \{C_3, \sigma_c\} + \{C_3^2, \sigma_b\}. \tag{5}$$

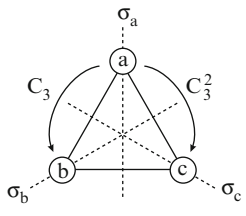

Fig. 2 Triatomic configuration with C_{3v} symmetry together with the corresponding symmetry labels

It is easily seen that the coset distribution reflects the generation of the triangle from the starting point on $\langle a \rangle$. The first coset is the set of all elements which map $\langle a \rangle$ onto itself, the second collects all elements which map $\langle a \rangle$ onto $\langle b \rangle$, and the third contains the elements which send $\langle a \rangle$ over into $\langle c \rangle$. There is thus a one-to-one mapping between the cosets and the elements of the orbit. The cosets thus really represent equivalent sites, and they too form an orbit. Through the coset expansion the geometric concept of equivalent nuclei may be turned into a purely group theoretical concept. We may now pass from a nuclear orbit to an electronic function space by decorating each site with an orbital which is totally symmetric under the respective stabilizer. The space of these basis functions transforms as the orbit of the nuclei, and its symmetry representation is called the *positional* representation [11, 12]. Again we may free ourselves of a particular set of nuclei and think of the positional representation as the transitive representation of the orbit of cosets of a particular site group. We will denote this orbit as $\Omega(H \subset G)$, and its representation as Γ_Ω. In the language of induction theory this positional or orbit representation corresponds to the induced representation from the totally symmetric subgroup representation:

$$\Gamma_\Omega = \Gamma \left(A' \, C_s \uparrow C_{3v} \right). \tag{6}$$

Although Γ_Ω describes a set of equivalent elements, it is not degenerate, since it can be further reduced into invariant subspaces. For the case of a triangle this representation gives rise to two irreducible representations (irreps) of C_{3v}.

$$\text{Triangle: } \Gamma_\Omega = A_1 + E. \tag{7}$$

Indeed the sum or trace of the elements of the orbit is certainly invariant under any group action, and thus always constitutes the totally symmetric root, A_1. In the present case the traceless reminder space with dimension 2 is in fact twofold degenerate. This is not always the case though. Already in a square this is no longer true as the positional representation of the four quadrangular sites, after subtraction of the A_1 irrep, further decomposes into $E + B_1$ irreps. The essential difference between the triangle and the square is that in the triangle the three sites are *equidistant*. This will prove to be a general result: a configuration of n equivalent sites gives rise to a degeneracy space of dimension $n - 1$, provided all sites are equidistant.

3.2 Doubly Transitive Orbits

As we have already indicated, in a group theoretical treatment the geometric concept of equivalent nuclei is generalized to the concept of equivalent site symmetries, which together constitute the orbit of cosets of a given subgroup. This is an essential point of the present treatment which allows us to make abstraction of the particular nuclear configuration and reformulate the problem entirely in group-theoretical terms. At this point we take a different route as compared to the first proof by Ruch

and Schönhofer, where the sites are identified as atomic nuclei. Let us consider equivalence inside the orbit $\Omega(H \subset G)$. In precise terms the orbit is *singly transitive*, meaning that there always exists a symmetry operation in G which can map a given coset $g_r H$ onto any other coset $g_s H$. To define degenerate irreps however a stronger criterion is needed, which requires the orbit of cosets to be *doubly transitive*. This means that any ordered pair of cosets can be mapped on any other ordered pair, i.e.:

$$\begin{aligned} &\forall\ g_r H, g_s H, g_u H, g_v H \in \Omega(H \subset G) \Rightarrow \\ &\quad \exists x \in G : x g_r H = g_u H\ \wedge\ x g_s H = g_v H. \end{aligned} \tag{8}$$

This criterion is a rigorous group theoretical translation of the intuitive concept of equal distances between all sites. As an example in a square there are no symmetry elements that will turn a pair of opposite sites into a pair of adjacent sites, which reflects the fact that the inter-site distances between opposite and adjacent sites are different. In contrast in a tetrahedron all vertices are equidistant and the six possible pairs or bonds can indeed be permuted. For the representation of a doubly transitive orbit the following theorem was proven by Hall: [13]

Theorem 1. *A doubly transitive permutation representation of a group G over the complex field is the sum of the identical representation and an absolutely irreducible representation [13].*

This theorem provides a connection between a degenerate irrep of dimension $n-1$ and the existence of an orbit of n equivalent and equidistant sites. We will express this result as follows:

$$\Gamma_\Omega = \Gamma_0 + \Gamma_{n-1}, \tag{9}$$

where the elements of the orbit are seen to transform according to the direct sum of two irreps: Γ_0 which is the totally symmetric irrep of G, and an irrep Γ_{n-1}, which represents a degeneracy of dimension $n-1$, i.e. one less than the dimension of the orbit. A legitimate example is the threefold degenerate T_2 irrep in a tetrahedron, which arises through the doubly transitive orbit of the C_{3v} subgroups:

$$\text{Tetrahedron: } \Gamma_\Omega = \Gamma\,(A_1\ C_{3v} \uparrow T_d) = A_1 + T_2. \tag{10}$$

A useful corollary, which was known to the Luleks, [14] reads:

Corollary 1. *The orbit of the cosets of a subgroup H of group G, $\Omega(H \subset G)$, can only be doubly transitive for H a maximal subgroup of G.*

A subgroup H is maximal if there are no intermediate subgroups between H and G in the branching scheme of G. A proof of this corollary is presented in the Appendix.

A case in point is the pentagonal subgroup D_{5d} of the icosahedral point group. This subgroup is a maximal subgroup, and the six pentagonal directions are 'equidistant', in the sense that any pair of them can be mapped onto any other pair. Induction then yields the five-fold degenerate H representation:

$$\text{Icosahedron: } \Gamma_\Omega = \Gamma\,(A_1\ D_{5d} \uparrow I_h) = A_{1g} + H_g\,. \tag{11}$$

Note that the opposite is not necessarily true, e.g. the orbit of a maximal subgroup is not necessarily doubly transitive. A case in point in icosahedral symmetry is the trigonal subgroup D_{3d}. This is a maximal subgroup, but its orbit is not doubly transitive. In fact an icosahedron has ten trigonal sites which are however not all equidistant. Induction from D_{3d} yields three irreps:

$$\text{Icosahedron: } \Gamma_\Omega = \Gamma\,(A_1\ D_{3d} \uparrow I_h) = A_{1g} + G_g + H_g\,. \tag{12}$$

It is also important to remind that double transitivity implies the mapping of all *ordered* pairs. As an example if the symmetry of the triangle is limited to C_3 only, the double transitivity is lost, since this group does not allow odd permutations that are needed to switch the ordering of pairs. As a result the E irrep is split into two complex conjugate one-dimensional irreps.

$$\Gamma_\Omega = \Gamma\,(A\ C_1 \uparrow C_3) = A + E_+ + E_-. \tag{13}$$

3.3 All-Transitive Orbits

When an ordered set of *all* n elements of a given orbit can be mapped onto any differently ordered set of these elements the orbit is *all-transitive* and the corresponding symmetry group will be isomorphic to the symmetric group, S_n which contains all permutations of n elements. In a 'molecular' sense, symmetric groups describe the symmetry of a set of n equivalent equidistant nuclei, which is a so-called simplex. The n-simplex is the elementary building block of a $n-1$ dimensional Euclidean space. The whole space can be tesselated in a lattice of such simplex unit cells. We have already encountered the triangle and tetrahedron as the simplexes of 2D and 3D space respectively. Their symmetry groups are isomorphic to symmetric groups:

$$\begin{aligned} C_{3v} &\sim S_3 \\ T_d &\sim S_4. \end{aligned} \tag{14}$$

The stabilizer of a vertex in a simplex, i.e. the group of all elements of S_n which leave a given vertex invariant, is the maximal subgroup S_{n-1}. The set of all vertices thus will transform as the induced representation of a totally symmetric irrep of the site group in the parent group. Since this representation is certainly doubly

Table 1 Isomorphism relations between the elements of the groups T_d and S_4

		T_d S_4	E 1^4	$8C_3$ $1^1 3^1$	$3C_2$ 2^2	$6S_4$ 4^1	$6\sigma_d$ $1^2 2^1$
A_1	(4)		1	1	1	1	1
A_2	(1^4)		1	1	1	−1	−1
E	(2^2)		2	−1	2	0	0
T_1	$(2, 1^2)$		3	0	−1	1	−1
T_2	(3, 1)		3	0	−1	−1	1

transitive, the theorem applies and the positional space contains a totally symmetric representation, denoted as (n), and a $n-1$ fold degenerate traceless irrep, Γ_{n-1}, which in the symmetric group is denoted as $(n-1, 1)$:

$$\Gamma_\Omega = \Gamma\left((n-1)\, S_{n-1} \uparrow S_n\right) = (n) + (n-1, 1). \tag{15}$$

The isomorphism between T_d and S_4 provides a simple illustration to become familiar with the formal description of permutational groups. A permutational operation on four elements can be characterized as a sequence of cyclic permutations, e.g. a threefold axis running through atom 1 will map 1 onto itself and produce a cyclic permutation of the remaining three atoms. It is therefore denoted as $(3, 1)$. All threefold elements have the same cycle structure and in view of the complete transitivity of the set thus must belong to the same symmetry classes. In this way the elements of T_d can easily be identified as S_4 operators, as shown in Table 1. The irreps themselves are also denoted as partitions of n, indicated between patentheses. Pictorially these partitions may be denoted by Young tableaux, as also indicated in the character table.

We may put the numbers from 1 to 4 in the Young tableaux in strictly increasing order, such that the number sequence in any row and in any column always increases. The number of ways in which this is possible gives the dimension of the corresponding irreducible representation. The important advantage of the symmetric group over the point groups is that the direct product rules as well as the corresponding Clebsch–Gordan coefficients can be obtained by general combinatorial formulae which apply to all symmetric groups [15]. As an example, the following product rules apply:

$$(n-1,1)\otimes(n-1,1)=\left[(n)+(n-1,1)+(n-2,1^2)\right]+\{(n-2,2)\}\,, \quad (16)$$

where square and round brackets denote the symmetrized and antisymmetrized products respectively.

4 Electronic Degeneracy

In the previous section the existence of a $n-1$ fold degeneracy was shown to be related to the presence of a set of n identical molecular sites, which are symmetry equivalent and equidistant from each other. In these cases the molecular point group can be considered to be a subgroup of the symmetric group S_n.

$$G \subset S_n. \quad (17)$$

The combinatorial structure of this parent group offers a closed form expression of the connection between permutational degeneracy and internal motion. This forms the basis of our proof.

4.1 Construction of a Degeneracy Basis

The theorem by Hall and its corollary provides us with a general tool to describe degenerate irreps of finite groups. The procedure proceeds as follows: one finds all maximal subgroups of a given group and then verifies if the orbit $\Omega(H \subset G)$ is doubly transitive. If this is the case, the theorem states the existence of a degenerate irrep, Γ_{n-1}, with dimension $n-1$. This link between Ω and Γ_{n-1} provides at once a carrier space which is singly and doubly transitive. This carrier space is a degeneracy basis, i.e. it defines a purely permutational description of the degeneracy manifold. Indeed for any function space, $|\Phi\rangle$, which transforms as Γ_{n-1}, symmetry lowering or subduction from G to H_a will yield exactly one component which is totally symmetric in the subgroup. Let us denote this component as $|\phi_a\rangle$, and define the other components by applying the coset generators to it, as follows:

$$g_r|\phi_a\rangle = |\phi_r\rangle. \quad (18)$$

The set $|\Phi\rangle = \{|\phi_i\rangle\}_{i=1,n}$ forms a carrier space which is in one to one correspondence with the elements of the orbit $\Omega(H \subset G)$. An orthogonal basis set for $|\Phi\rangle$ may then always be defined by forming the $n-1$ traceless combinations of these n components. As an example in the case of a tetrahedron an arbitrary function space, transforming as T_2, will have exactly one component which is totally symmetric under a C_{3v} subgroup, and which we will label as $|\phi_a\rangle$. Four such components can be formed, one for each trigonal site. The T_2 basis may then be expressed (up to

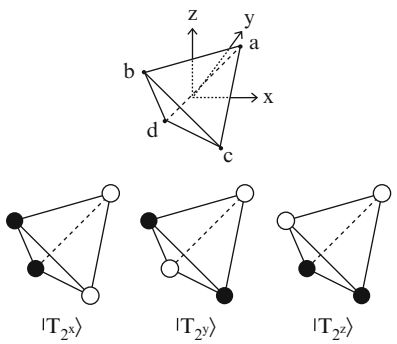

Fig. 3 The threefold degenerate T_2 representation and the tetrahedron

Table 2 Degeneracies in the cubic and icosahedral groups

D_3	$\Gamma\,(A_1\ C_2 \uparrow D_3) = A_1 + E$
O	$\Gamma\,(A_1\ D_4 \uparrow O) = A_1 + E$
	$\Gamma\,(A_1\ D_3 \uparrow O) = A_1 + T_1$
	$\Gamma\,(A_2\ D_3 \uparrow O) = A_2 + T_2$
I	$\Gamma\,(A\ T \uparrow I) = A_1 + G$
	$\Gamma\,(A_1\ D_5 \uparrow I) = A_1 + H$

a common normalizer) as three orthogonal traceless combinations of this standard basis (cf. Fig. 3):

$$
\begin{aligned}
|T_2x\rangle &= \frac{1}{2}\left(|\phi_a\rangle - |\phi_b\rangle + |\phi_c\rangle - |\phi_d\rangle\right)\\
|T_2y\rangle &= \frac{1}{2}\left(|\phi_a\rangle - |\phi_b\rangle - |\phi_c\rangle + |\phi_d\rangle\right)\\
|T_2z\rangle &= \frac{1}{2}\left(|\phi_a\rangle + |\phi_b\rangle - |\phi_c\rangle - |\phi_d\rangle\right).
\end{aligned}
\tag{19}
$$

Extension of this method to the alternative tetrahedral threefold degenerate irrep T_1 is straigthforward. This irrep is formed in the same way as T_2 but starting from the antisymmetric A_2 representation in the C_{3v} subgroup, hence:

$$
\Gamma\,(A_2\ C_{3v} \uparrow T_d) = A_2 + T_1. \tag{20}
$$

When this method is applied to the point group degeneracies, a distinction must be made between spherical-like point groups, which include the cubic and icosahedral families, and the cylindrical-like point groups which contain the cyclic and dihedral families. The application to the first class is shown in Table 2. In this case nearly all degeneracies stem from doubly transitive orbits of maximal subgroups. The only exceptions are the threefold degenerate irreps in the icosahedral point group. These would require the presence of a maximal subgroup of order 30 which is not available in I_h.

On the other hand for the cylindrical-like point groups only the simplest case with triangular symmetry, obeys the equidistance criterion required by the present construction. This case is included in Table 2 as D_3. In summary the expansion of a degenerate manifold in a permutational carrier space based on maximal subgroups can be executed for all degenerate irreps of the cubic and icosahedral groups, except for the T irreps in the icosahedron. For the cyclic groups double transitivity does not exist, except for the triangle. However in this case there is the additional feature that single transitivity is of a cyclic nature, requiring only one generator. So here too the concept of a permutational carrier space will simplify the analysis. This aspect will be developed in Sect. 6.1.

4.2 Construction of the Jahn–Teller Hamiltonian

At present we have found that for the degenerate point group irreps which are listed in the table the basis functions can be expressed by means of a carrier space which exactly matches the orbit of a maximal subgroup of the point group, and counts $|G|/|H| = n$ elements. The one-particle Hamiltonian operating in this carrier space can easily be constructed as follows:

$$\mathrm{H} = k \sum_{i<j} \left(|\phi_i\rangle\langle\phi_j| + |\phi_j\rangle\langle\phi_i| \right), \tag{21}$$

where as previously the i and j components refer to elements of the orbit $\Omega(H \subset G)$. Since this orbit is doubly transitive the interaction parameter k does not depend on the pair indices. The Hamiltonian contains $n(n-1)/2$ symmetrized inter-site operators. As the theorem states the Γ_Ω representation of the carrier space corresponds to the direct sum $\Gamma_0 + \Gamma_{n-1}$. The symmetrized square of this direct sum not only covers the symmetries of the inter-site operators but also of the on-site diagonal operators of type $|\phi_i\rangle\langle\phi_i|$. The latter transform as the representation of Γ_Ω itself. The inter-site operators thus span the symmetrized square of the positional representation minus Γ_Ω:

$$\begin{aligned} \Gamma_\mathrm{H} &= [\Gamma_\Omega \otimes \Gamma_\Omega] - \Gamma_\Omega \\ &= [(\Gamma_0 + \Gamma_{n-1}) \otimes (\Gamma_0 + \Gamma_{n-1})] - \Gamma_\Omega \\ &= [\Gamma_{n-1} \otimes \Gamma_{n-1}] . \end{aligned} \tag{22}$$

Note in the second line of this equation that symmetrization of the direct square gives rise to only one cross-term. This equation expresses the standard Jahn–Teller result that time-even interactions in a degeneracy space transform according to the symmetrized square (indicated by square brackets) of the corresponding irrep. This square can be further resolved, into a non-distortive totally symmetric part and the proper Jahn–Teller part.

We will now take this result to the parent symmetric group, which describes the permutation of all the sites. In this group the sites transform as $(n-1,1)$ and the inter-site operators span the symmetrized square of $(n-1,1)$, hence:

$$\Gamma_{\mathrm{H}} = [(n-1,1) \otimes (n-1,1)]\,. \tag{23}$$

This square can be further resolved, yielding:

$$\Gamma_{\mathrm{H}} = (n) + (n-1,1) + (n-2,2). \tag{24}$$

The non-totally symmetric interactions which can appear in the degenerate $(n-1,1)$ irrep thus will transform as $(n-1,1) + (n-2,2)$.

So far the analysis has lead to the concept of a carrier space which links the degeneracy to a doubly transitive orbit of cosets of maximal subgroups. Interactions in this space are expressed as transition operators between the cosets. The final part of the treatment should bring in the vibrational degrees of freedom which are responsible for the Jahn–Teller activity.

5 Vibrational Degrees of Freedom

5.1 Symmetric Group Analysis

Having identified the symmetries of the electronic distortion operators, we now determine the symmetries of the nuclear degrees of freedom. These are defined as the direct product of the positional representation with the symmetry of the translations [12, 16]. The n-simplex is situated in a $(n-1)$-dimensional space and thus will exhibit $(n-1)$ translations. The corresponding irrep is denoted as Γ_T. One easily realizes that this will correspond to the $(n-1,1)$ irrep: from the center of the simplex one can move in n different directions, but the vectorial sum of all these directions amounts to zero, hence the translational space has one degree of freedom less than the number of sites. The direct product can be decomposed in a standard way as follows:

$$\Gamma_{\Omega} \otimes \Gamma_T = (n) + 2(n-1,1) + (n-2,2) + (n-2,1^2). \tag{25}$$

These degrees of freedom also contain the so-called external degrees of freedom: translations and rotations. The rotations, described by Γ_R, transform as the anti-symmetrized square of the translations. One thus has for the external modes:

$$\begin{aligned} \Gamma_T &= (n-1,1) \\ \Gamma_R &= \{\Gamma_T \otimes \Gamma_T\} = (n-2,1^2). \end{aligned} \tag{26}$$

Finally the symmetries of the internal or vibrational degrees of freedom are obtained by subtracting the external modes from the space of nuclear motions:

$$\Gamma_\Omega \otimes \Gamma_T - \Gamma_T - \Gamma_R = (n) + (n-1,1) + (n-2,2). \tag{27}$$

Clearly this symmetry shows a perfect match with the symmetry of the interaction Hamiltonian, as obtained in (24).

$$\Gamma_\Omega \otimes \Gamma_T - \Gamma_T - \Gamma_R \equiv \Gamma_{\mathrm{H}}. \tag{28}$$

This expression is the central result of our paper and the most concise expression of the Jahn–Teller theorem. It shows that the time-even interactions in a degenerate irrep based on a simplex of n nuclei are in one-to-one correspondence with the vibrational degrees of freedom of that simplex. Another way to express this is that the bonds between the sites form a complete set of internal coordinates. In 3D this reflects the Cauchy theorem that 'in a convex polyhedron with rigid faces the angles between the faces will also be rigid' [17, 18].

As in the original treatment of Jahn and Teller our result attributes the vibronic instability to the terms in the Hamiltonian which are linear in the nuclear displacements. Higher order contributions will of course occur as well but they cannot be responsible for the conical instability at the high symmetry origin.

5.2 Extensions to Other Symmetries and irreps

The case of a perfect match which we have considered in the previous section reveals the intimate connection between degeneracy and vibrational degrees of freedom. In the simplex this connection attains a one-to-one correspondence. In more complex frames the connection is often disguised by the presence of additional inactive modes. In fact five possible situations can occur, depending on the relationship between the space of normal modes and the space of JT interactions. The symmetries of the non-totally symmetric vibronic interactions will be denoted as Γ_{JT}, while the symmetries of the non-totally symmetric normal modes will be denoted as Γ_{NM}. The five possible set relations between these two sets are:

$$\begin{aligned}
&1.\ \Gamma_{JT} = \Gamma_{NM} \\
&2.\ \Gamma_{JT} \subset \Gamma_{NM} \\
&3.\ \Gamma_{JT} \cap \Gamma_{NM} = \emptyset \\
&4.\ \Gamma_{JT} \cap \Gamma_{NM} \neq \emptyset \\
&5.\ \Gamma_{JT} \supset \Gamma_{NM}.
\end{aligned} \tag{29}$$

The first case describes the perfect match of both spaces, which as we have seen occurs for the $(n-1,1)$ irrep of the n-simplex.

The usual JT effect in 3D point groups exemplifies the second case, $\Gamma_{JT} \subset \Gamma_{NM}$. These cases involve molecules that are more involved than the simplexes, which implies that the site which is stabilized by a maximal subgroup contains more nuclei than the one that is considered in the simplex. As a result all the possible JT interaction symmetries are represented *at least* by one normal mode, but in addition the space of vibrational modes also contains inactive modes. A case in point are centrosymmetric molecules where only *gerade* modes can be JT active, the odd modes are found in the remainder space $\Gamma_{NM} - \Gamma_{JT}$.

The third case, $\Gamma_{JT} \cap \Gamma_{NM} = 0$, constitutes an exception to the Jahn–Teller theorem since it states that none of the normal modes has the right symmetry to couple with the degeneracy. As we know this occurs in linear molecules. More examples can be found in higher dimensions.

The remaining cases offer the intriguing possibility that not all of the vibronic operators that are required for the coupling between the sites have a counterpart in the space of normal modes. This does not occur in point group symmetries, although in practice coupling to some modes may be so weak that it can be neglected, thus giving rise to partial Jahn–Teller activity. Again in higher symmetric groups examples of these cases may be found. They occur for degenerate irreps that do not subduce one-dimensional subrepresentations when symmetry is lowered to the maximal subgroup of the site symmetry. This implies that the electronic structure on the sites is of a composite nature.

6 Applications

6.1 2D: Cylindrical Symmetry

As we have indicated before, apart from the triangle, orbits which correspond to the sites of higher polygons are not doubly transitive. In this case Halls theorem cannot be used. However as was already alluded to in the original proof of Jahn and Teller, for such cylindrical like structures, there is a general generic treatment, which in its simplest form only is based on the cyclic generator structure of these polygons. In a n-cycle symmetry eigenfunctions can always be written as cyclic waves running over the sites, with some angular momentum λ, i.e.:

$$\Psi_\lambda = \sum_k \exp(\lambda \frac{2\pi k i}{n})|k\rangle, \tag{30}$$

where λ is an integer ring quantum number, which characterizes the symmetry of this function. When the function is rotated over an angle of $2\pi/n$ a phase factor of $\exp(-\lambda \frac{2\pi i}{n})$ appears. Unless $\lambda = n/2$, this wave function will always have a complex conjugate counterpart which has the same electronic density over the sites, and thus will be degenerate. This implies that the vibronic instability resides in the

electronic operator connecting Ψ_λ and $\Psi_{-\lambda}$. It is given by:

$$|\Psi_{-\lambda}\rangle\langle\Psi_\lambda| = \sum_{k,k'} \exp(\lambda \frac{2\pi(k+k')i}{n})|k\rangle\langle k'|. \tag{31}$$

When this operator is rotated over the angle $2\pi/n$ a phase is built up which equals $\exp(-2\lambda\frac{2\pi i}{n})$, hence the operator runs twice as fast as the wavefunctions. Its symmetry is therefore characterized by the ring quantum number 2λ.

A convenient set of internal normal modes is offered by the set of all edges of the polygon. The set of n-edges transforms as the regular representation, thus it offers a complete set of all irreducible representations of the cyclic generator. As a result this set will always contain the symmetry of the active operator.

6.2 3D: The Icosahedral Quintuplet

The fivefold degenerate representation of the icosahedral group is the highest possible orbital degeneracy within the 3D point groups. As indicated in (11), this fivefold degeneracy originates from the presence of six equivalent and equidistant pentagonal directions in the icosahedron (labeled A to F in Fig. 5). The mere existence of this quintuplet is remarkable in itself and can be related to a unique property of its parental symmetric group S_6. The symmetric group S_6 stands out in the family of symmetric groups S_n as it is the only member which has two non-equivalent maximal subgroups of type S_{n-1} (S_5) [19]. As the icosahedral group $I \cong A_5 \subset S_5 \subset S_6$, this will lead to two separate branches in the subgroup lattice leading to inequivalent icosahedral embeddings as indicated in Fig. 4. To fully understand these two embeddings, it is helpfull to take a closer look at the exact structure of their intermediate S_5 subgroups.

A first type of S_5 subgroup can easily be seen to originate from fixing one of the elements of S_6 and acting fully transitive on the remaining five elements. This type of S_{n-1} subgroup is common to all S_n groups, but clearly not the one we are interested in as it does not act doubly transitive, not even singly transitive, on the set of six pentagonal directions. The icosahedral quintuplet therefore originates from a second and unexpected branch in the subgroup lattice of S_6. In this branch the embedding of I into S_6 is mediated by a second type of S_5 subgroup (see Table 3) which acts doubly transitive on the six pentagonal directions. The actual elements of

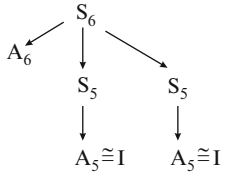

Fig. 4 Branching scheme of the symmetric group S_6 showing two separate branches leading to inequivalent I subgroups

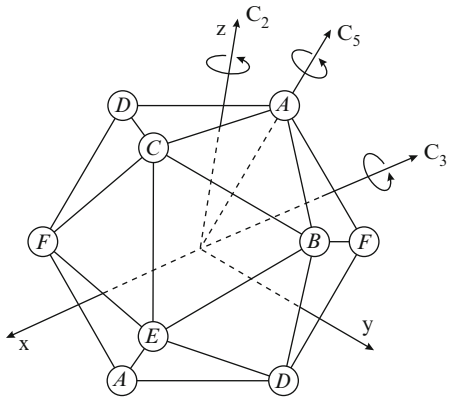

Fig. 5 The icosahedron showing the six equidistant pentagonal directions A to F and the three generators of (32)

Table 3 Embedding of the icosahedral group I into the symmetric group S_6

S_6	1	15	40	45	90	120	144	15	90	40	120
	1^6	$1^4 2^1$	$1^3 3^1$	$1^2 2^2$	$1^2 4^1$	$1^1 2^1 3^1$	$1^1 5^1$	2^3	$2^1 4^1$	3^2	6^1
S_5	1			15	30		24	10		20	20
	1^6			$1^2 2^2$	$1^2 4^1$		$1^1 5^1$	2^3		3^2	6^1
$I \cong A_5$	E			$15C_2$			$12C_5$			$20C_3$	
							$12C_5^2$				

this icosahedral subgroup can easily be deducted using the three generators depicted in Fig. 5:

$$\begin{aligned} C_5 &\to (A)(B, F, E, D, C) \\ C_3 &\to (A, B, F)(C, D, E) \\ C_2 &\to (A, C)(B, D)(E)(F). \end{aligned} \tag{32}$$

In order to generate the intermediate S_5 subgroup it suffices to add one of its uneven permutations to the generators of I. As seen from Table 3 the uneven permutations constitute three classes: 6^1, 2^3 and $1^2 4^1$ with respectively 30 ,10 and 20 elements. Prototypical examples are:

$$\begin{aligned} 6^1 &\to (A, C, F, E, D, B) \\ 2^3 &\to (A, E)(C, D)(F, B) \\ 1^2 4^1 &\to (A)(B)(C, D, F, E). \end{aligned} \tag{33}$$

The action of these elements can be clarified by means of the icosahedral embedding of Fig. 5. From the 120 possible 6^1 elements existing within S_6, only those encircling a 'supertriangle' of the icosahedron survive within S_5. A supertriangle is by definition composed of a triangular face of the icosahedron together with its three neigboring faces. The 6^1 element listed above for instance originates

from encircling the supertriangle AFD in Fig. 5 (in an anticlockwise direction). Obviously the number of such supertriangles coincides with the number of triangular faces of the icosahedron therefore leading to exactly twenty elements of type 6^1. Notice that the chosen sense of rotation is immaterial as the set of permutations generated by clockwise rotations would be exactly the same due to the inversion symmetry of Fig. 5. The ten elements of the class 2^3 are now easily identified as cubes of these 6^1 elements. The squares of the 6^1 elements do not constitute a new class. They are of even type and coincide nicely with the twenty C_3 rotations of the icosahedral group. The last uneven class $1^2 4^1$ consists of elements which fix two pentagonal directions and cyclicly permute the remaining four elements. Only thirty from a total of ninety such elements survive in the subduction from S_6 to S_5. They correspond to those elements for which the four non-fixed elements encircle two neighboring triangles on the surface of the icosahedron. For the listed $1^2 4^1$ element for instance the fourcyle (C, D, F, E) encircles the neighboring triangles CDF and FEC.

In previous work we have shown how this embedding of the icosahedron in S_6 can be used to resolve the product multiplicity in the icosahedral $H \otimes (g + 2h)$ Jahn–Teller problem [10, 20]. In the context of atomic spectroscopy, Judd and Lo have made use of the S_6 connection to explain some puzzling degeneracies in the spectroscopic terms of d^3 [21].

As a further illustration we will demonstrate here the use of this embedding to resolve a multiplicity case for the symmetry coordinates of a vibrating icosahedron [22]. An icosahedral cage with twelve atoms has 30 internal modes. Since the icosahedron is a deltahedron, the stretchings of the 30 edges form a non-redundant set of internal coordinates. The corresponding symmetry representations are given by:

$$\Gamma_{NM} = a_g + t_{1u} + t_{2u} + g_g + g_u + 2h_g + h_u. \tag{34}$$

For the even modes, displacements of opposite edges are equal. If two opposite edges are being squeezed simultaneously, two pentagonal directions approach each other. In this way the 15 pairs of opposite edges correspond to the 15 edges of the S_6 simplex, consisting of the six pentagonal directions. Hence the 15 gerade symmetry coordinates will transform in S_6 as $(6) + (5, 1) + (4, 2)$, exactly as described in (27). Using the embedding relations in Table 3, the following subduction relations between the S_6 and I_h labels can be found:

$$\begin{aligned} (6) &\rightarrow A_g \\ (5, 1) &\rightarrow H_g \\ (4, 2) &\rightarrow G_g + H_g. \end{aligned} \tag{35}$$

This subduction shows that the two equisymmetric h_g cluster deformations may be distinguished by a different S_6 parentage. The construction of the modes with $(5, 1)$ and $(4, 2)$ parentage proceeds as follows. One first defines a carrier space of H_g symmetry, based on the six pentagonal sites. The components of this space are labeled $\theta, \epsilon, \xi, \eta, \zeta$.

$$|\theta\rangle = \frac{1}{2}(-|A\rangle + |D\rangle - |E\rangle + |F\rangle)$$

$$|\epsilon\rangle = \frac{1}{\sqrt{12}}(|A\rangle - 2|B\rangle - 2|C\rangle + |D\rangle + |E\rangle + |F\rangle)$$

$$|\xi\rangle = \frac{1}{\sqrt{2}}(|D\rangle - |F\rangle)$$

$$|\eta\rangle = \frac{1}{\sqrt{2}}(-|A\rangle + |E\rangle)$$

$$|\zeta\rangle = \frac{1}{\sqrt{2}}(-|B\rangle + |C\rangle). \tag{36}$$

Then these components are coupled using Clebsch–Gordan coefficients for the $H \otimes H = 2H$ direct product. In view of the product multiplicity in this coupling, two independent sets of coefficients exists. The coefficients which we have published before are based on a product multiplicity separation which obeys the S_6 parentage [23]. The published a and b coefficients correspond to the $(4, 2)$ and $(5, 1)$ Young tableaux resp. Hence by using these components we obtain at once the desired permutational multiplicity separation. Upon coupling only the off-diagonal terms are kept, since these correspond to the inter-site distances. Here we will limit ourselves to present the normalized coordinates for pentagonal and trigonal distortion modes. In the coordinate frame of Fig. 5, the h_g-symmetry components which are totally symmetric along the pentagonal C_5 direction, corresponding to site A, are given by:

$$\begin{aligned} Q_{5,1} = \frac{1}{\sqrt{30}}(&2r_{AB} + 2r_{AC} + 2r_{AD} + 2r_{AE} + 2r_{AF} \\ &- r_{BC} - r_{BD} - r_{BE} - r_{BF} - r_{CD} - r_{CE} - r_{CF} - r_{DE} - r_{DF} - r_{EF}) \\ Q_{4,2} = \frac{1}{\sqrt{10}}(&-r_{BC} + r_{BD} + r_{BE} - r_{BF} - r_{CD} + r_{CE} + r_{CF} \\ &- r_{DE} + r_{DF} - r_{EF}) . \end{aligned} \tag{37}$$

Here the r variables denote the distance between two pentagonal directions, which correspond to the simultaneous activation of the two edges connecting the atoms along these directions. Note that the $Q_{5,1}$ coordinate corresponds to a pure pentagonal squashing mode: the icosahedron is elongated along the A direction, and simultaneously compressed around its waist. The $Q_{4,2}$ mode behaves differently. This mode does not involve the apical A site. The two pentagonal rings forming the tropics around the waist are compressed, while the 10 edges in between those rings are elongated. The components which gives rise to a trigonal distortion oriented along the C_3 direction in Fig. 5 are given by:

$$Q_{5,1} = \frac{1}{\sqrt{6}}(r_{AB} + r_{AF} + r_{BF} - r_{CD} - r_{CE} - r_{DE})$$
$$Q_{4,2} = \frac{1}{\sqrt{18}}(2r_{AD} + 2r_{BE} + 2r_{CF} - r_{AB} - r_{AF} - r_{BF} - r_{CD} - r_{CE} - r_{DE}). \tag{38}$$

Here the roles are switched. Now the $Q_{4,2}$ mode describes a pure trigonal squash, which elongates the icosahedron along the C_3 direction. The $Q_{5,1}$ behaves differently: three sites A, B, F are pushed away from each other while the three remaining sites C, D, E approach each other.

6.3 4D: The Hyperoctahedron

Blount indicated that in higher dimensions the Jahn–Teller theorem not necessarily holds [7]. We will illustrate this here for the case of the hyperoctahedron, which is a 4D polytope. The symmetry of this structure can easily be constructed by straightforward generalization of the octahedral group in 3D. A 3D octahedron is composed of six vertices, arranged symmetrically around the origin along the three Cartesian directions, i.e. at: $\pm x, \pm y, \pm z$. The 48 operations of the group O_h corresponds to all interchanges of these six vertices that obey the following rules:

All transpositions of vertices on the same axis, e.g. $(+x) \leftrightarrow (-x)$
All permutations of the three directions, e.g. $(\pm x) \leftrightarrow (\pm y) \leftrightarrow (\pm z)$

The first rule gives rise to a group of eight elements corresponding to Z_2^3, where Z_2 is the cyclic group of order two. The corresponding point group is the D_{2h} normal subgroup of the octahedron. The second rule consists of 6 permutations of three objects, as described by the symmetric group S_3. The combination of both gives rise to a so-called wreath product of Z_2^3 and S_3, which is isomorphic to O_h:

$$O_h = {Z_2}^3 \times S_3. \tag{39}$$

The elements of the octahedral group will permute the six vertices and as such be part of the full permutation group S_6. The octahedral group is a subgroup of S_6, since not all permutations are in accordance with the rules, e.g. it is not allowed by the rules to interchange $(+x)$ and $(+z)$, without simultaneously interchanging $(-x)$ and $(-z)$.

This presentation of the octahedral symmetry group can directly be extended to the hyperoctahedron [24, 25]. This will be a 4D polytope, formed by eight vertices, distributed evenly over the four Cartesian directions, i.e. $\pm x, \pm y, \pm z, \pm u$. The hyperoctahedral group, commonly denoted as W_4 from the German *Würfel* which signifies dice, is given by:

$$W_4 = {Z_2}^4 \times S_4. \tag{40}$$

This group contains 384 elements. It contains 20 classes, which may be labeled by a combination of the labels from the parent symmetry group S_8 and the permutational subgroup S_4. The corresponding character table is available from the literature and will be reproduced in Table 4 for convenience [25]. In order to obtain the normal modes of the hyperoctahedron we first derive the positional representation of the eight vertices. Since the S_8 labels refer to permutations of the eight vertices, the character of the positional representation will simply correspond to the number of 1-cycles in each class. These numbers indeed indicate how many vertices are left invariant by the symmetry operations in that class. The symmetry of the translations can also easily be derived, since it must correspond to a 4-dimensional irrep, which subduces the T_{1u} symmetry in the O_h subgroup. The only irrep with these properties is $\Gamma_1^{(4)}$. The antisymmetrized square of this irrep is equal to $\Gamma_1^{(6)}$ and corresponds to the symmetry of the rotational degrees of freedom. Hence one has for the normal modes:

$$\begin{aligned} \Gamma_\Omega &= \Gamma_1^{(1)} + \Gamma_1^{(3)} + \Gamma_1^{(4)} \\ \Gamma_\Omega \otimes \Gamma_1^{(4)} - \Gamma_T - \Gamma_R &= \Gamma_1^{(1)} + \Gamma_1^{(3)} + \Gamma_1^{(4)} + \Gamma_3^{(6)} + \Gamma_1^{(8)}. \end{aligned} \tag{41}$$

There are two twofold degenerate irreducible representations, $\Gamma_i^{(2)}, i = 1, 2$. Their squares both yield the same result:

$$\Gamma_i^{(2)} \times \Gamma_i^{(2)} = \{\Gamma_3^{(1)}\} + [\Gamma_1^{(1)} + \Gamma_1^{(2)}]. \tag{42}$$

It is immediately clear that the non-totally symmetric part of the symmetrized square, which transforms as $\Gamma_1^{(2)}$ is not contained in the normal modes of the hyperoctahedron. This simply signifies that there are no Jahn–Teller distortions in this case. The twofold degenerate irreps of the hyperoctahedron thus constitute a 4D example of an exception, exactly as the 1D case. The subgroup structure of W_4 may be invoked to explain this result. In order to obtain a twofold degenerate irrep by a double transitive orbit one would need a subgroup of one third of the total group order, i.e. 128. Clearly W_4 does not contain such a subgroup. Since the total order is given by $2^4 \times 4!$, a subgroup of order 128 can only be obtained by the wreath product of Z_2^4 with a subgroup of S_4 that would have to be of order 8. But S_4 does not contain such a subgroup, hence W_4 cannot be divided in an orbit of rank 3.

Even more interesting results can be obtained for irreducible representations of dimension three: $\Gamma_i^{(3)}, i = 1, 3$. In this case the antisymmetrised and symmetrised parts of the square are given by:

$$\Gamma_i^{(3)} \times \Gamma_i^{(3)} = \{\Gamma_1^{(6)}\} + [\Gamma_1^{(1)} + \Gamma_1^{(3)} + \Gamma_2^{(6)}]. \tag{43}$$

This case corresponds to the fifth possibility in (29) which does not occur in lower dimensions and exemplifies a partial overlap between the Jahn–Teller modes and the normal modes. In order to destroy the symmetry of this level one would need modes of type $\Gamma_1^{(3)}$ and $\Gamma_2^{(6)}$. A glance at the normal modes of the hyperoctahedron

Table 4 Character table of the hyperoctahedral group W_4

S_8	1^8	$2^1 1^6$	$4^1 1^4$	$1^4 2^2$	$1^4 2^2$	$6^1 1^2$	$4^1 2^1 1^2$	$2^3 1^2$	$2^3 1^2$	$3^2 1^2$	8^1	4^2	4^2	$4^1 2^2$	$4^1 2^2$	$6^1 2^1$	$3^2 2^1$	2^4	2^4	2^4
S_4	1^4	1^4	$2^1 1^2$	$2^1 1^2$	1^4	$3^1 1$	$2^1 1^2$	$2^1 1^2$	1^4	$3^1 1^1$	4^1	4^1	2^2	2^2	$2^1 1^2$	$3^1 1^1$	$3^1 1^1$	2^2	$2^1 1^2$	1^4
	1	4	12	12	6	32	24	24	4	32	48	48	12	24	12	32	32	12	12	1
O_h	E	σ_h	C_4	σ_d	C_2	S_6	S_4	C_2'	i	C_3										
$\Gamma_1^{(1)}$	1	1	1	1	1	1	1	1	1	1	1	1	1	1	1	1	1	1	1	1
$\Gamma_2^{(1)}$	1	−1	−1	1	1	−1	1	−1	−1	1	−1	1	1	−1	−1	1	−1	1	1	1
$\Gamma_3^{(1)}$	1	1	−1	−1	1	1	−1	−1	1	1	−1	−1	1	1	−1	1	1	1	−1	1
$\Gamma_4^{(1)}$	1	−1	1	−1	1	−1	−1	1	−1	1	1	−1	1	−1	1	1	−1	1	−1	1
$\Gamma_1^{(2)}$	2	2	0	0	2	−1	0	0	2	−1	0	0	2	2	0	−1	−1	2	0	2
$\Gamma_2^{(2)}$	2	−2	0	0	2	1	0	0	−2	−1	0	0	2	−2	0	−1	1	2	0	2
$\Gamma_1^{(3)}$	3	3	1	1	3	0	1	1	3	0	−1	−1	−1	−1	1	0	0	−1	1	3
$\Gamma_2^{(3)}$	3	−3	−1	1	3	0	1	−1	−3	0	1	−1	−1	1	−1	0	0	−1	1	3
$\Gamma_3^{(3)}$	3	3	−1	−1	3	0	−1	−1	3	0	1	1	−1	−1	−1	0	0	−1	−1	3
$\Gamma_4^{(3)}$	3	−3	1	−1	3	0	−1	1	−3	0	−1	1	−1	1	1	0	0	−1	−1	3
$\Gamma_1^{(4)}$	4	2	2	2	0	1	0	0	−2	1	0	0	0	0	−2	−1	−1	0	−2	−4
$\Gamma_2^{(4)}$	4	−2	−2	2	0	−1	0	0	2	1	0	0	0	0	2	−1	1	0	−2	−4
$\Gamma_3^{(4)}$	4	2	−2	−2	0	1	0	0	−2	1	0	0	0	0	2	−1	−1	0	2	−4
$\Gamma_4^{(4)}$	4	−2	2	−2	0	−1	0	0	2	1	0	0	0	0	−2	−1	1	0	2	−4
$\Gamma_1^{(6)}$	6	0	2	0	−2	0	0	−2	0	0	0	0	2	0	2	0	0	−2	0	6
$\Gamma_2^{(6)}$	6	0	−2	0	−2	0	0	2	0	0	0	0	2	0	−2	0	0	−2	0	6
$\Gamma_3^{(6)}$	6	0	0	2	−2	0	−2	0	0	0	0	0	−2	0	0	0	0	2	2	6
$\Gamma_4^{(6)}$	6	0	0	−2	−2	0	2	0	0	0	0	0	−2	0	0	0	0	2	−2	6
$\Gamma_1^{(8)}$	8	4	0	0	0	−1	0	0	−4	−1	0	0	0	0	0	1	1	0	0	−8
$\Gamma_2^{(8)}$	8	−4	0	0	0	1	0	0	4	−1	0	0	0	0	0	1	−1	0	0	−8

shows that only the first one of these is included in the normal modes. No distortion operators exist with $\Gamma_2^{(6)}$ symmetry, hence the degeneracy can only be partially lifted.

7 Epikernel Principle and Dynamic Symmetry

The permutational proof also elucidates two important general properties of JT potentials: the epikernel principle, and the symmetry of the dynamic ground state.

The epikernel principle was originally proposed as an simple rule to predict the preferential symmetry of a Jahn–Teller distortion [26]. Later on it was rationalized using the technique of the isostationary function [27]. Epikernels are those subgroups of the point group that occur in the distortion space formed by the Jahn–Teller active coordinates. The lowest subgroup of the epikernel set is called the kernel. A Jahn–Teller distortion cannot lower the symmetry of a compound below the kernel symmetry. As an example an e_g vibration of an octahedron cannot lower the symmetry below the kernel group D_{2h}, which is a normal subgroup of O_h. Thus any modal point in the twofold distortion space will at least have orthorhombic symmetry. In addition the e_g distortion space contains three preferential directions where a tetragonal symmetry axis is conserved. Along these directions the symmetry is D_{4h} which is an epikernel of the distortion space. According to the epikernel principle stable minima on a Jahn–Teller distortion prefer epikernel rather than kernel points. According to the present proof this principle is a natural consequence of the structure of electronic degeneracies. A degeneracy is built on a doubly transitive orbit, and as we have seen such an orbit is based on *maximal* subgroups of a group. These naturally correspond to the maximal epikernels. The Jahn–Teller coordinates correspond to the intersite interactions between these epikernel directions.

When dynamics is taken into account the Jahn–Teller distortion starts to move inside the nuclear frame, and the complex gradually runs through all equivalent sites of the orbit on which the degeneracy is built. According to Bersuker and Pollinger the ground state of such a system has a dynamic symmetry which as a rule exhibits the same type of degeneracy as the electronic symmetry which was at the origin of the Jahn–Teller effect [28]. The connection with the present proof is obvious: an electronic $n-1$-fold degeneracy is based on an orbit of n sites, which correspond to the stable minima of the JT potential. In the symmetric group based on permutations of these minima, the eigenvectors span the positional representation of these minima, and thus will transform as the totally symmetric representation, and the $(n-1)$ basic vector irrep, which is precisely the symmetry of the electronic degeneracy. When the coupling to the $(n-2,2)$ modes becomes more important the symmetry of the dynamic ground state may change, and this behavior indeed may occur in the icosahedral quintuplet case, with dominant trigonal coupling [29]. (See also [30])

8 Conclusion

In this treatment we have searched the underlying common structure that unites all Jahn–Teller problems. The starting point has been the important theorem by Hall, which relates the existence of an $(n-1)$-fold degeneracy to a doubly transitive orbit of n elements. This yields a simple permutational proof for nearly all cubic and icosahedral degeneracies as well for the degeneracies in a triangle. Exceptional cases are the T_1 and T_2 irreps in an icosahedron for which no doubly transitive orbit exist, since there is no subgroup of rank 4 in the icosahedral group. Apart from the triangle, higher order polygons, which all belong to subgroups of cylindrical symmetry, also do not contain doubly transitive orbits.

The induction processes which we have used in the present treatment were mainly limited to inductions from totally symmetric roots in the subgroups. Induction from non-totally symmetric subgroup irreps sometimes give rise to interesting alternative constructions of degeneracies, which may clarify the kaleidoscope structure [31] of the icosahedral T irreps, and allow extensions into spin degeneracies.

Acknowledgements A.C. is indebted to Prof. T. Lulek (Rzeszów) for pointing out Halls theorem, and to Prof. H. Köppel (Heidelberg) for interesting discussions. This work was supported by the Flemish Government through the concerted action scheme. E.L. is research fellow from the National Science Fund FWO.

Appendix

In this appendix we prove the corrolary to the theorem of Hall that the orbit of the cosets of a subgroup H of group G can only be doubly transitive for H a maximal subgroup of G. To this end we consider a further subgroup $S \subset H$, and examine if the orbit of cosets of S can be doubly transitive. Let g_r and h_ρ denote cosets representatives of H in G, and S in H resp., i.e.:

$$G = \sum_{r}^{|G|/|H|} g_r H$$
$$H = \sum_{\rho}^{|H|/|S|} h_\rho S. \tag{44}$$

The cosets of S in G may then be generated by the product of both types of generators:

$$G = \sum_{r,\,\rho}^{|G|/|S|} g_r h_\rho S. \tag{45}$$

Elements of this orbit are thus labeled by double labels (r, ρ). If we want this orbit to be doubly transitive the elements of G should be able to effectuate any mapping between pairs of such labels. It can easily be shown that this is not the case. Take for example the case where g_r is the unit element e, and consider the initial pair $(e, \rho), (e, \sigma)$. Both these cosets thus belong to H. Now we wonder if there would exist an element g_x that maps this pair onto a pair $(e, \rho'), (r, \sigma')$. In this target pair the first coset stays in H, but the second is outside H.

$$? \exists\, g_x : g_x h_\rho S = h_{\rho'} S \quad \wedge \quad g_x h_\sigma S = g_r h_{\sigma'} S \tag{46}$$

Clearly such an element cannot be found. Indeed from the first requirement it follows that g_x must be in H, while the second condition places g_x outside H. Hence only maximal subgroups can have doubly transitive cosets.

References

1. H.A. Jahn, E. Teller, Proc. R. Soc. **A161** 220 (1937)
2. I.B. Bersuker, *The Jahn–Teller Effect* (Cambridge University Press, Cambridge, 2006)
3. E. Ruch, Z. Elektrochemie **61** 913 (1957)
4. T. Sato, K. Tokunaga, N. Iwahara, K. Shizu, K. Tanaka. *in: The Jahn-Teller Effect – Advances and Perspectives. Springer series in Chemical Physics* (Springer, Berlin, 2009)
5. A. Ceulemans, P. W. Fowler, M. Szopa, Math. Proc. R. Ir. Acad. **98A** 139 (1998)
6. E. Ruch, A. Schönhofer, Theor. Chim. Acta (Berl.) **3** 291 (1965)
7. E.I. Blount, J. Math. Phys. **12** 1890 (1971)
8. I.V.V. Raghavacharyulu. J. Phys. C Solid State Phys. **6** L455 (1973)
9. V.I. Pupyshev, Int. J. Quantum Chem. **107** 1446 (2007)
10. A. Ceulemans, E. Lijnen, Bull. Chem. Soc. Jpn. **80** 1229 (2007)
11. T. Lulek, Acta Physica Pol. **A57** 407 (1980)
12. A. Ceulemans, Mol. Phys. **54** 161 (1985)
13. M. Hall, *The Theory of Groups* (Macmillan, New York, 1959)
14. B.Lulek, T. Lulek, J. Phys. A: Math. Gen. **17** 3077, 1984
15. M. Hamermesh, *Group Theory and its Application To Physical Problems* (Addison-Wesley, Reading MA, 1962)
16. T. Lulek, M. Szopa, J. Phys. A: Math. Gen. **23** 677, (1990)
17. A. Ceulemans, P.W. Fowler, Nature **353** 52, 1991
18. A.L. Cauchy, J. Ecole Impériale Polytech. **19** 87 (1813)
19. B. Newton, B. Benesh, J. Algebra **304** 1108 (2006)
20. E. Lijnen, A. Ceulemans, Europhys. Lett. **80** 67006 (2007)
21. E. Lo, B.R. Judd, Phys. Rev. Lett. **82** 3224 (1999)
22. A. Ceulemans, B.C. Titeca, L.F. Chibotaru, I. Vos, P.W. Fowler, J. Phys. Chem. A **105** 8284 (2001)
23. P.W. Fowler, A. Ceulemans, Mol. Phys. **54** 767 (1985)
24. P. W. Fowler, A. Rassat, A. Ceulemans, J. Chem. Soc. Faraday Trans. **92** 4877, (1996)
25. M. Baake, B. Gemünden, R. Oedinger, J. Math. Phys. **23** 944 (1982)
26. A. Ceulemans, L.G. Vanquickenborne, Struct. Bonding (Berlin) **71** 125 (1989)
27. A. Ceulemans, J. Chem. Phys. **87** 5374 (1987)
28. I.B. Bersuker, V.Z. Polinger, *Vibronic Interactions in Molecules and Crystals* (Springer, Berlin, 1989)

29. C.P. Moate, M.C.M. O'Brien, J.L. Dunn, C.A. Bates, Y.M. Liu, V.Z. Polinger, Phys. Rev. Lett. **77** 4362 (1996)
30. F.S. Ham, C.H. Leung, *The Unpublished Work of F.S. Ham on the Jahn–Teller Effect*. (Trinity Enterprise Inc, Saint-John NB, 2008)
31. B.R. Judd, E.Lo, J. Phys. B **32** 1073 (1999)

http://www.springer.com/978-3-642-03431-2

The Jahn-Teller Effect
Fundamentals and Implications for Physics and Chemistry
Köppel, H.; Yarkony, D.R.; Barentzen, H. (Eds.)
2009, XXI, 915 p., Hardcover
ISBN: 978-3-642-03431-2